

ARTICLE

Open Access

The orphan nuclear receptor *Nr4a1* mediates perinatal neuroinflammation in a murine model of preterm labor

Sarah M. Estrada¹, Andrew S. Thagard¹, Mary J. Dehart², Jennifer R. Damici², Elisabeth M. Dornisch², Danielle L. Ippolito³, Irina Burd⁴, Peter G. Napolitano⁵ and Nicholas Ieronimakis²

Abstract

Prematurity is associated with perinatal neuroinflammation and injury. Screening for genetic modulators in an LPS murine model of preterm birth revealed the upregulation of *Nr4a1*, an orphan nuclear transcription factor that is normally absent or limited in embryonic brains. Concurrently, *Nr4a1* was downregulated with magnesium sulfate (MgSO₄) and betamethasone (BMTZ) treatments administered to LPS exposed dams. To understand the role of *Nr4a1* in perinatal brain injury, we compared the preterm neuroinflammatory response in *Nr4a1* knockout (KO) versus wild type (wt) mice. Key inflammatory factors *Il1b*, *Il6* and *Tnf*, and Iba1+ microglia were significantly lower in *Nr4a1* KO versus wt brains exposed to LPS in utero. Treatment with MgSO₄/BMTZ mitigated the neuroinflammatory process in wt but not *Nr4a1* KO brains. These results correspond with a reduction in cerebral hemorrhage in wt but not mutant embryos from dams given MgSO₄/BMTZ. Further analysis with *Nr4a1-GFP-Cre* × *tdTomato loxP* reporter mice revealed that the upregulation of *Nr4a1* with perinatal neuroinflammation occurs in the cerebral vasculature. Altogether, this study implicates *Nr4a1* in the developing vasculature as a potent mediator of neuroinflammatory brain injury that occurs with preterm birth. It is also possible that MgSO₄/BMTZ mitigates this process by direct or indirect inhibition of *Nr4a1*.

Introduction

Preterm delivery and the long-term impacts on the developing neonate remain a major concern for obstetric care in the United States. The rate of preterm birth in the United States continue to rise¹. Though our understanding of preterm birth and the associated fetal complications continues to evolve, there is still much to address. The pathogenesis of preterm birth and its consequences is complex and multifactorial, likely resulting from numerous elements including intrauterine

inflammation and dysregulation of fetal neurodevelopmental processes^{2,3}.

Preterm delivery, particularly when earlier in gestation, is linked to a high prevalence of cognitive impairment, developmental delays, and central nervous system disorders, such as cerebral palsy (CP)^{4,5}. Perinatal brain injury is thought to result from acute neuroinflammation, driven by an excess of cytokines and immunological responses^{2,6}. Treatment aimed at reducing perinatal neuroinflammation includes magnesium sulfate (MgSO₄), which is thought to reduce vascular instability, decrease pro-inflammatory cytokines, and/or prevent hypoxic injury and ischemia-induced tissue damage⁶. Although the underlying molecular mechanisms of MgSO₄ remain poorly understood, antenatal use has been shown to decrease the incidence of CP. Several randomized controlled trials have demonstrated improved outcomes with

Correspondence: Nicholas Ieronimakis (nicholas.m.ieronimakis.civ@mail.mil)


¹Department of Obstetrics and Gynecology, Division of Maternal Fetal Medicine, Madigan Army Medical Center, Tacoma, WA, USA

²Department of Clinical Investigation, Madigan Army Medical Center, Tacoma, WA, USA

Full list of author information is available at the end of the article.

Edited by B. Joseph

© This is a U.S. government work and not under copyright protection in the U.S.; foreign copyright protection may apply 2020

 **Open Access** This article is licensed under a Creative Commons Attribution 4.0 International License, which permits use, sharing, adaptation, distribution and reproduction in any medium or format, as long as you give appropriate credit to the original author(s) and the source, provide a link to the Creative Commons license, and indicate if changes were made. The images or other third party material in this article are included in the article's Creative Commons license, unless indicated otherwise in a credit line to the material. If material is not included in the article's Creative Commons license and your intended use is not permitted by statutory regulation or exceeds the permitted use, you will need to obtain permission directly from the copyright holder. To view a copy of this license, visit <http://creativecommons.org/licenses/by/4.0/>.

MgSO₄, particularly for preterm pregnancies treated before 32–34 weeks gestation^{7–12}. However, the effectiveness of MgSO₄ is not guaranteed with an estimated number needed to treat of 56¹³.

In conjunction with MgSO₄, antenatal corticosteroids such as betamethasone (BMTZ), have also improved fetal outcomes. Trials using corticosteroids in preterm labor have demonstrated reductions in intracranial hemorrhage and cystic periventricular leukomalacia^{14,15}. Corticosteroids are characteristically anti-inflammatory and may alleviate the fetal neuroinflammatory burden with prematurity. Analogous to MgSO₄, the exact molecular mechanisms of corticosteroids remain unclear¹⁶. If the mechanisms of injury and the actions of these treatments are delineated, other interventions may be developed.

We sought to identify pro-inflammatory targets that are responsive to MgSO₄ and BMTZ treatments. Using microarray screening, we identified the upregulation of *Nr4a1* in a murine model of preterm labor. *Nr4a1* is an orphan nuclear receptor, also known as Nur77, TR3, and NGFI-B, that has been implicated in a variety of immune responses and adult neuroinflammatory injury^{17–20}. In the prenatal brain, *Nr4a1* expression is limited and not required for normal development^{21–23}. Based on these preliminary findings, we hypothesized that *Nr4a1* plays an important role in perinatal brain injury and sought to characterize its role using mutant mouse models. Our primary objective was to evaluate the neuroinflammatory response of *Nr4a1* knockout (KO) versus wild type (wt) mice. Additionally, we sought to evaluate the relationship between *Nr4a1* KO and wt mice in conjunction with MgSO₄ and BMTZ treatments. Finally, we used Cre-loxP fate mapping to identify the cellular expression of *Nr4a1* that is upregulated in response to perinatal neuroinflammation.

Materials and methods

Animal models

All animal experiments and procedures were approved by the Institutional Animal Care and Use Committee. Animals were randomly selected to receive treatments in all experiments/groups and the data acquisition/analysis was performed blinded with coded samples. For the microarray screening, CD-1 mice were purchased from Charles River Laboratories (Wilmington, MA, USA) and on E15.5 received an intrauterine injection of 100 µl containing 100 µg lipopolysaccharide (LPS) from *Escherichia coli* O55:B5 (Sigma-Aldrich, St. Louis, MO, USA) or the vehicle (PBS)²⁴. Mice were subsequently treated with normal saline (NS) or MgSO₄/BMTZ, 30 min post-injection of LPS/PBS. MgSO₄ and BMTZ treatments were administered subcutaneously as previously described²⁵. Brains were harvested 6 h following the intrauterine injections and frozen immediately in liquid nitrogen for

expression analysis. Sample sizes were estimated based on cytokine gene expression from previous studies^{26,27}.

Nr4a1 KO and wt controls on a C57BL/6 background were acquired from The Jackson Laboratory (Bar Harbor, ME, USA)²². Once acclimated (2 weeks), males and females were paired by their respective genotypes: KO male with KO female and wt male with wt female. Pregnancy was confirmed by the presence of a vaginal plug at which time males were separated from the females. At E15.5, females received a 100 µl intrauterine injection of either the PBS vehicle or 250 µg of LPS. The higher LPS dose was chosen for this and subsequent experiments in order to evaluate a more severe neuroinflammatory response that has been reported for the C57BL/6 strain²⁸. A second group of wt and *Nr4a1* KO mice received LPS or PBS and subsequent treatment with MgSO₄/BMTZ as previously described. Embryos were again collected 6 h following the intrauterine injections. In these experiments, brains were harvested from half of the embryos for expression analysis while the remainder were placed in formalin, cut sagittal and embedded in paraffin.

For fate mapping, *Nr4a1-GFP-Cre* recombinase and *tdTomato loxP* reporter mice were acquired from The Jackson Laboratory; strains *C57BL/6-Tg(Nr4a1-EGFP/cre820Khog/J* and *B6.Cg-Gt(ROSA)26Sortm14(CAG-tdTomato)Hze/J* respectively. The *Nr4a1-GFP-Cre* allele enables the expression of green fluorescent protein (GFP) and Cre simultaneously under the *Nr4a1* promoter²⁹. The *tdTomato loxP* allele (Ai14 variant) is irreversibly activated in the presence of Cre³⁰. Offspring with both alleles were generated by mating *Nr4a1-GFP-Cre* males with *tdTomato loxP* females. Dams received a 100 µl intrauterine injection of either 250 µg LPS or the PBS vehicle. In these experiments, only LPS exposed mice received MgSO₄/BMTZ. Six hours post-intrauterine injections, embryo brains were initially fixed by maternal cardiac perfusion. First, the right ventricle was punctured to permit drainage and then 10 ml PBS followed by 10 ml 4% formaldehyde were infused into the left ventricle³¹. Embryos were then placed in 5 ml 4% formaldehyde for an additional 2 h and then dehydrated with a sucrose gradient beginning with 10%, 20%, and then 30%, in which they were left overnight at 4 °C. The next day embryos were cut sagittal and frozen in optimal cutting temperature (OCT) compound.

Microarray

RNA isolation

While working on dry ice, individual CD-1 embryo brains were selected and transferred to a pre-chilled 2.0 ml tube containing one 5 mm stainless steel bead (Qiagen, Germantown, MD, USA). Once brains were transferred, 700 µl of QIAzol Lysis Reagent (Qiagen) was added to each sample. Samples were immediately

homogenized using a TissueLyzer LT (Qiagen) for 5 min at 50 Hz, then placed at -80°C until all samples were processed. RNA was extracted using the miRNeasy 96 kit (Qiagen), according to the manufacturer's instructions. The quantity of RNA samples was evaluated with a multichannel Nanodrop 8000 spectrophotometer (Thermo Fisher, Waltham, MA, USA).

Gene array

With an input of 100 ng total RNA, hybridization-ready, fragmented, labeled, sense-stranded DNA targets were prepared using Affymetrix GeneChip® WT Plus Reagent Kit (Affymetrix, Santa Clara, CA, USA). We then prepared the labeled cDNA targets, trays, and arrays with the GeneTitan Hybridization, Wash and Stain Kit for WT array plates (Affymetrix). Samples were then applied to the Mouse Gene 2.1 ST 96 Array Plate and placed in the GeneTitan System (Affymetrix). These steps conformed to the manufacturer's recommendations. Of the 96 arrays, 80 passed the GeneTitan scanning quality control which includes visual inspection and QC metrics provided by the Affymetrix Expression Console (hybridization control performance, labeling control performance, internal control gene performance, signal histogram, probe cell intensity, Pearson's Correlation, and Spearman Rank Correlation). In order to verify the performance of the replicates, Pearson's R^2 was manually calculated for each set of replicates within each group. The 16 which did not meet criteria were repeated. All 16 repeats passed quality control and were included in the final analysis.

Gene array data analysis

We normalized arrays using an extension of the *PLIER* (Probe Logarithmic Intensity Error) algorithm, called the iterPLIER procedure, in the Affymetrix Expression Console. The iterPLIER (gene level) procedure discards feature sets that perform poorly, as described by Qu et al.³². We imported the resulting CHP files into Partek Genomics Suite version 6.12.0907 (St. Louis, Missouri, USA). Affymetrix library files included all available reference files related to MoGene-2_1-st. To determine differentially expressed genes, an analysis of variance (ANOVA) was conducted with contrasts. Gene lists were generated by applying a cutoff by Benjamini-Hochberg False Discovery Rate ($\text{FDR} < 0.05$)^{33,34}.

qRT-PCR

E15.5 brains were snap frozen in liquid nitrogen and subsequently processed for gene expression analysis. Whole brains were homogenized and then RNA was extracted utilizing the RNeasy Lipid Tissue Kit (Qiagen), following the manufacturer instructions. First strand cDNA was then generated using the GoScript reverse transcription kit (Promega, Fitchburg, WI, USA). PCR

reactions were conducted with SYBR Green on a Light Cycler 480 II system (both from Roche, Indianapolis, IN, USA). Reactions were performed in triplicate for each gene sample using the following conditions: $95^{\circ}\text{C} \times 5$ min, then 40 cycles at $95^{\circ}\text{C} \times 10$ s, $60^{\circ}\text{C} \times 10$ s, and $72^{\circ}\text{C} \times 10$ s. The relative expression of each respective target was calculated by ΔCt , normalizing to ribosomal protein *18s*^{35,36}. Primer sequences for *Foxd1* were generated using NCBI primer-BLAST³⁷. With exceptions to *18s* and *Foxd1*, the majority of primers sequences were generated by the Harvard PrimerBank³⁸. Primer sequences are detailed in Supplementary Table S1.

Histology

Sagittal sections from whole embryos placed in formalin or OCT were cut $8\ \mu\text{m}$ thick. Formalin fixed paraffin embedded sections were cleared and used for Iba1 immunohistochemical staining. Antigen retrieval was performed using citrate buffer pH 6.0 (Vector Laboratories, Burlingame, CA, USA) for 25 min at 95°C . Slides were blocked with biotin/streptavidin (Vector Laboratories) in accordance with the manufacturer's instructions and then with 2.5% Horse serum (Vector Laboratories) for 1 h. Washes were performed with PBS + 0.05% Tween 20 and a polyclonal goat anti-Iba1 (Abcam ab107159, Burlingame, CA, USA) was added at 1:1000 overnight at 4°C in PBS + 0.05% Tween 20 with 1% BSA. The next day, an anti-goat pre-diluted ready to use secondary (Vector Laboratories) was applied for 1 h, followed by DAB staining. Slides were counterstained with hematoxylin and Iba1+ cells were quantified within $20\times$ fields of fetal brains using the ImageJ cell counter application. The mean number of Iba1+ cells was calculated relative to the dimensional area of our microscopes $20\times$ objective ($358\ \text{mm}^2$). Paraffin slides were also cleared and stained with hematoxylin and eosin (H&E) to visualize pathology. The frequency of cerebral hemorrhage was counted, either present or absent from at least three fields for each brain³⁹. Frozen slides were examined under fluorescence to identify GFP and tdTomato reporters. Sections were stained for GFP to enhance the signal⁴⁰. For this a polyclonal chicken anti-GFP (Abcam ab13970) was added at 1:1000 for 1 h, followed by a donkey anti-chicken secondary conjugated to Alexa Fluor 488 (Jackson ImmunoResearch, West Grove, PA, USA), also at 1:1000 for 1 h. Tissues were counterstained with DAPI and biotinylated BS1 (Vector Laboratories) at 1:500 for 1 h and followed by streptavidin Alexa Fluor 647 (Jackson ImmunoResearch) at 1:1000 for 1 h. All images were captured on a Leica (Buffalo Grove, IL, USA) SP8 system with DFC7000 camera. The brightness and contrast for fluorescent images were adjusted evenly between experimental and control samples to reduce background.

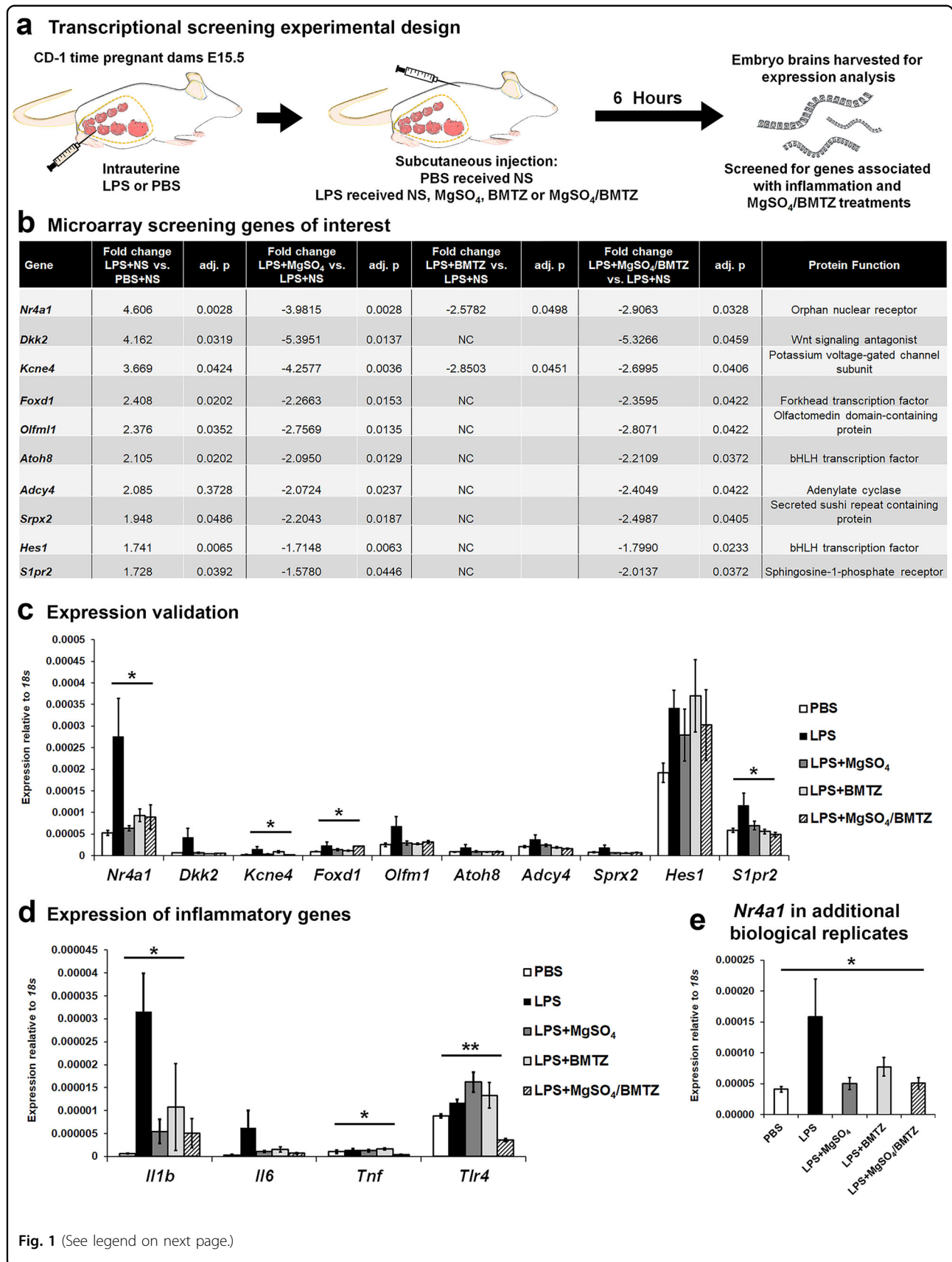


Fig. 1 (See legend on next page.)

(see figure on previous page)

Fig. 1 Screening for inflammatory regulators reveals the upregulation of *Nr4a1*. **a** CD-1 dams were randomized to receive an intrauterine injection of LPS or PBS at E15.5. Dams given LPS were randomized to receive subcutaneous injections of a combination of MgSO₄ and/or BMTZ or the normal saline (NS) vehicle control. Mice that received PBS received NS. Brains were harvested for gene expression analysis 6 h following intrauterine injections. **b** The top genes upregulated with LPS and downregulated with treatment. Fold changes represent genes upregulated with LPS+NS groups vs. PBS+NS controls (column 2) and downregulated in LPS groups with MgSO₄ (column 4), BMTZ (column 6), or the combination of MgSO₄/BMTZ (column 8). Column 10 denotes a description of each gene. NC denotes no change. This comparison represents *N* = 4 embryo brains per condition, analyzed by microarray. **c** Validation by qRT-PCR in the same samples used for microarray analysis in **b**. **d** Expression of key inflammatory genes (*Il1b*, *Il6*, *Tnf* and *Tlr4*) by qRT-PCR, in the same samples assayed in **b**. **e** Additional embryo brains (total *N* = 8–9 per group) analyzed by qRT-PCR to confirm the upregulation of *Nr4a1*. **p* < 0.05 and ***p* < 0.005 by one-way ANOVA. Error bars represent ±SEM.

Statistics

With exception to the aforementioned microarray analysis, gene expression comparisons were accomplished with either unpaired Student's *t*-test or one-way ANOVA with and without Tukey's post-hoc test. Categorical data (Figs. 5, 6) was analyzed by chi-squared test using the PBS or PBS + MgSO₄/BMTZ control groups as the expected reference. These comparisons were conducted using either Excel (Microsoft, Redmond, WA, USA) or SPSS (IBM, Armonk, NY, USA). Graphs and tables were generated using Excel.

Results

Nr4a1 expression is upregulated with perinatal neuroinflammation

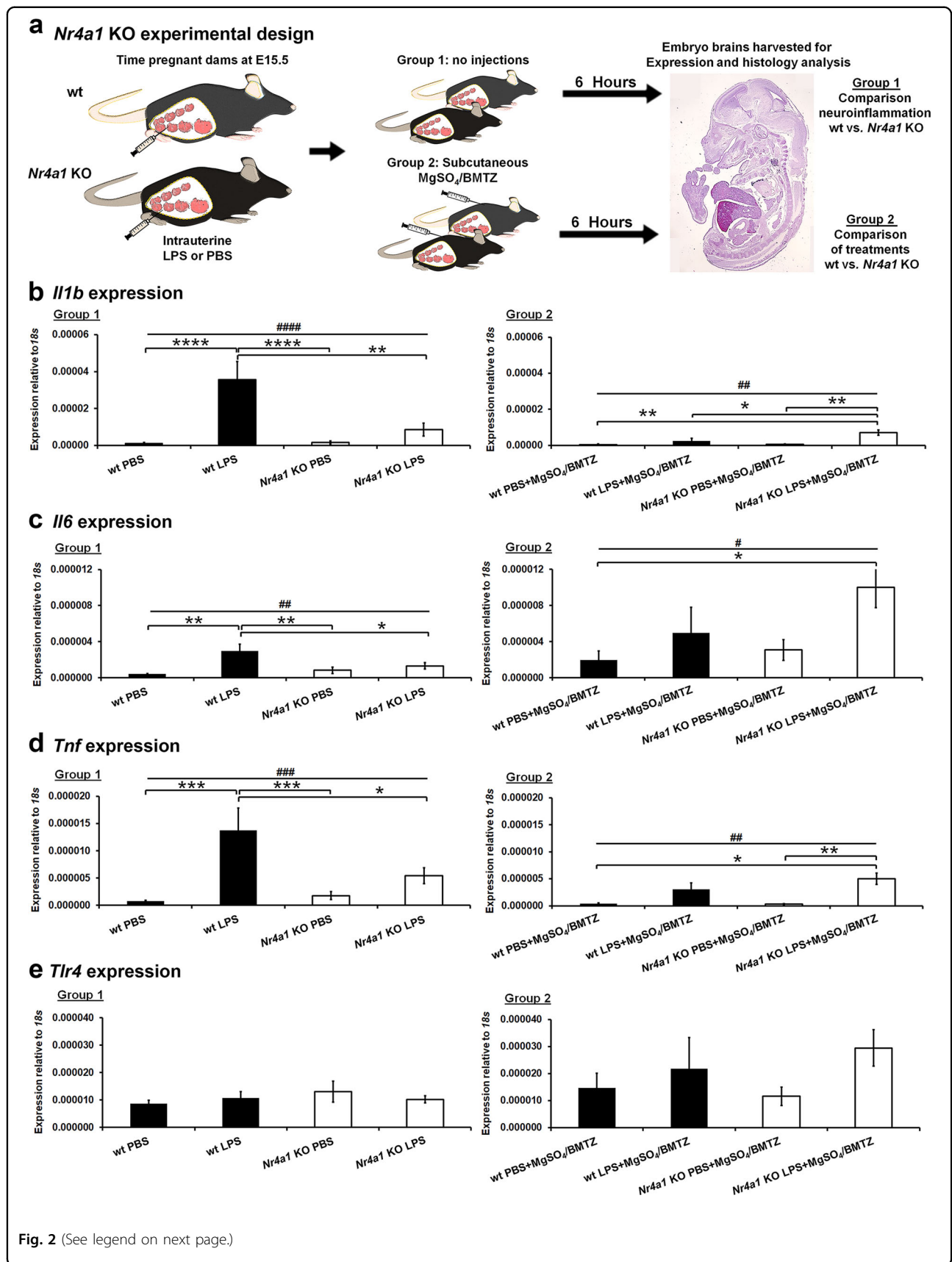
To identify mediators of perinatal brain injury, we utilized microarray analysis to screen for inflammation-associated genes differentially expressed with LPS exposure and modulated by treatment with MgSO₄, BMTZ, or the combination of MgSO₄/BMTZ (Fig. 1a). The top ten genes upregulated with LPS injections and downregulated with at least one treatment were selected for further validation based on the degree of fold change and adjusted *p*-value. These genes included transcription factors (*Nr4a1*, *Foxd1*, *Atoh8*, *Hes1*), regulatory proteins (*Dkk2*, *Olfml1*, *Srpx2*, *Kcne4*), an enzyme (*Adcy4*) and a cell surface receptor (*Slpr2*) (Fig. 1b)^{41–50}. Only *Nr4a1*, *Kcne4*, *Foxd1*, and *Slpr2* were significantly higher with LPS and similar to controls with treatments by qRT-PCR (Fig. 1c). The observed changes corresponded with the significant upregulation of proinflammatory genes: *Interleukin 1 beta* (*Il1b*), *Tumor necrosis factor* (*Tnf*), and *Toll-like receptor 4* (*Tlr4*) (Fig. 1d)^{26,51}. Expression of *Interleukin 6* (*Il6*) was also elevated with LPS, although not significantly. In comparison to LPS alone, treatment with any combination of MgSO₄ and/or BMTZ resulted in lower expression of these inflammatory factors. Interestingly, we observed an increase of *Tlr4* with LPS and either treatment administered individually. With the treatment combination, the expression of *Tlr4* was similar to PBS controls. From this screening and validation, we identified *Nr4a1* as the most prominent gene modulated by LPS and treatments. Validation in additional samples supported this result (Fig. 1e).

Nr4a1 KO mice show significant reductions in perinatal neuroinflammation and injury

In order to assess whether *Nr4a1* regulates perinatal neuroinflammatory injury, we compared KO mice versus wt controls. Second, we compared LPS injury in wt and KO mice with the administration of MgSO₄ and BMTZ to evaluate if the protective effects of these treatments are related to *Nr4a1*. The therapies of both MgSO₄ and BMTZ were chosen due to their effectiveness when given in combination versus individual administration (Fig. 1d, e). These experiments were split into two groups, one evaluating LPS alone and a second comparing treatments. Group 1 consisted of wt and *Nr4a1* KO mice that received only LPS or PBS. Group 2 consisted of wt and *Nr4a1* KO mice that received LPS or PBS and MgSO₄/BMTZ treatment (Fig. 2a). Although MgSO₄ and BMTZ are relatively safe, their administration in PBS controls was included to account for any effects that may occur in mutant mice.

Once more, to evaluate the perinatal neuroinflammatory response to LPS we examined the expression of *Il1b*, *Il6*, *Tnf*, and *Tlr4* (Fig. 2b). Gene expression analysis by qRT-PCR revealed a robust upregulation of cytokines in wt versus *Nr4a1* KO fetal brains with LPS. The expression of *Il1b*, *Il6*, and *Tnf* in the wt brains was significantly elevated in the LPS group as compared to the PBS control (Fig. 2b, d, Group 1). In the *Nr4a1* KO brains, the expression of these cytokines was similar between PBS and LPS exposed animals. With the addition of MgSO₄/BMTZ treatment, the wt inflammatory response was significantly lower than with LPS alone (Fig. 2b, d, Group 2). In contrast, the *Nr4a1* KO mice exposed to LPS showed greater expression of *Il1b* with LPS in comparison to PBS controls versus wt brains. Expression of *Il6* and *Tnf* cytokines was also higher in *Nr4a1* KO brains exposed to LPS and MgSO₄/BMTZ, but only between certain treatment groups (Fig. 2c, d, Group 2).

In addition to gene expression, we also compared the cellular response to neuroinflammation by quantifying the number of Iba1+ microglia. With LPS, a greater number of Iba1+ cells was observed in wt embryo brains (Fig. 3a)^{52,53}. No difference was observed in the brains of *Nr4a1* KO embryos with PBS or LPS exposure. With



(see figure on previous page)

Fig. 2 Examination of perinatal inflammation in the absence of *Nr4a1*. **a** Experimental design comparing wild type (wt) and *Nr4a1* knockout (KO) dams exposed to perinatal neuroinflammation at E15.5. Two groups of animals were evaluated; one comparing only PBS vs. LPS and a second comparing PBS vs. LPS with subsequent treatments of MgSO₄/BMTZ. Embryo brains were harvested for molecular analysis, at 6 h following intrauterine injections of PBS or LPS. **b–e** Expression analysis for principal inflammatory genes *Il1b*, *Il6*, *Tnf*, and *Tlr4* was examined in E15.5 brains. This analyses represents per condition $N = 13–17$ brains for group 1 and $N = 7–12$ brains for group 2. [#] $p < 0.05$, ^{##} $p < 0.005$, ^{###} $p < 0.0005$ by one-way ANOVA and ^{*} $p < 0.05$, ^{**} $p < 0.005$, ^{***} $p < 0.0005$, ^{****} $p < 0.00005$ by Tukey's post-hoc test. Error bars represent \pm SEM.

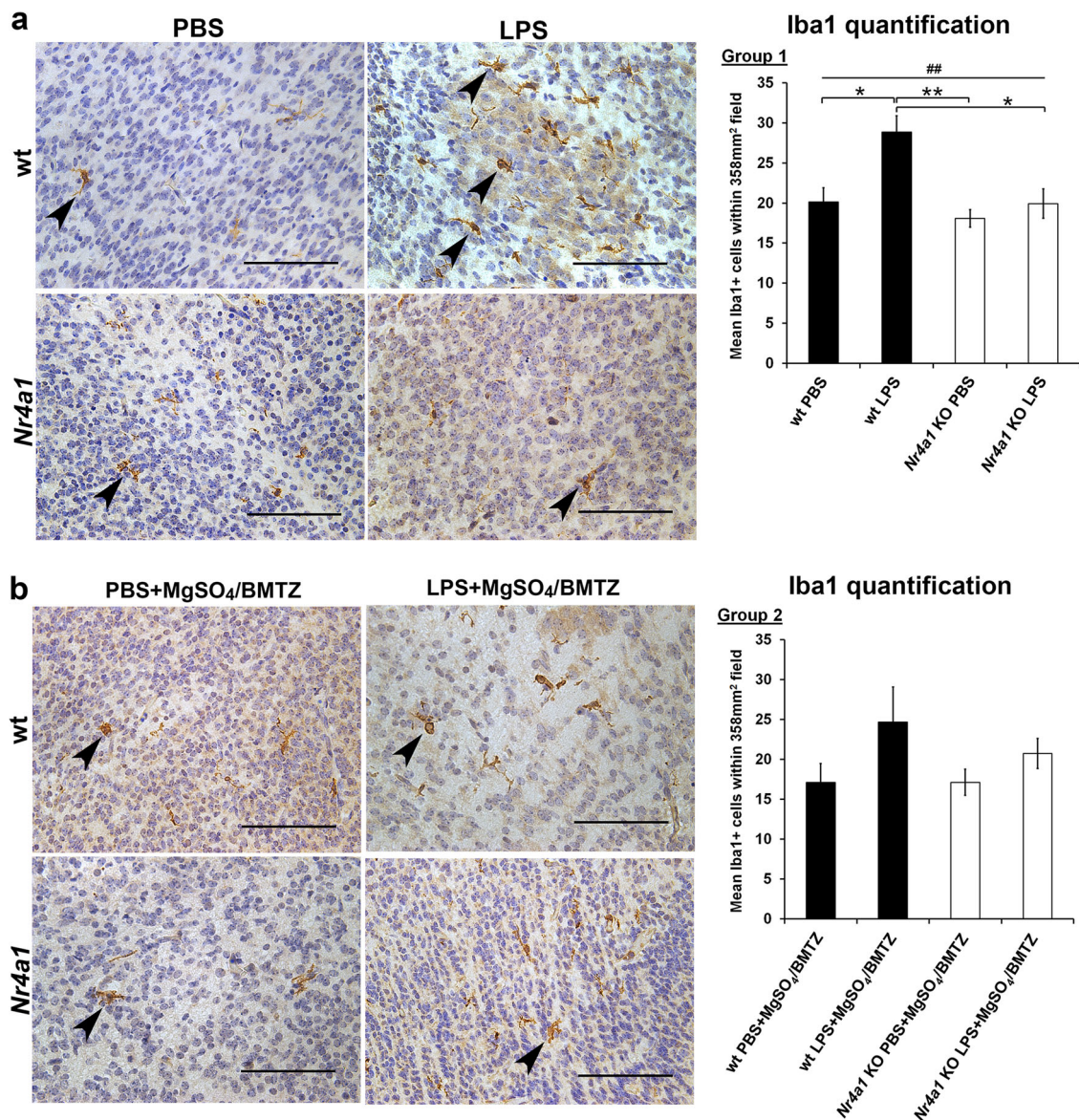


Fig. 3 Microglial comparison between wt and *Nr4a1* KO embryos. E15.5 brains from wt and *Nr4a1* KO embryos were stained for Iba1 with DAB (brown). Sections were counterstained with hematoxylin to visualize nuclei in blue and high magnification micrographs (40 \times) depict Iba1+ microglia (arrowheads) between conditions. Cell quantifications graphed to the right were conducted at a lower magnification (20 \times) in order to reduce error. **a** Comparison and quantification of Iba1+ cells for group 1 ($N = 6$ brains per condition); wt and *Nr4a1* KO animals were exposed to PBS or LPS. **b** Comparison and quantification for group 2 ($N = 3$ brains per condition); wt and *Nr4a1* KO animals were exposed to PBS or LPS and MgSO₄/BMTZ treatment. Scale bars denote 100 μ m. ^{##} $p < 0.005$ by one-way ANOVA and ^{*} $p < 0.05$, ^{**} $p < 0.005$, by Tukey's post-hoc test. Error bars represent \pm SEM.

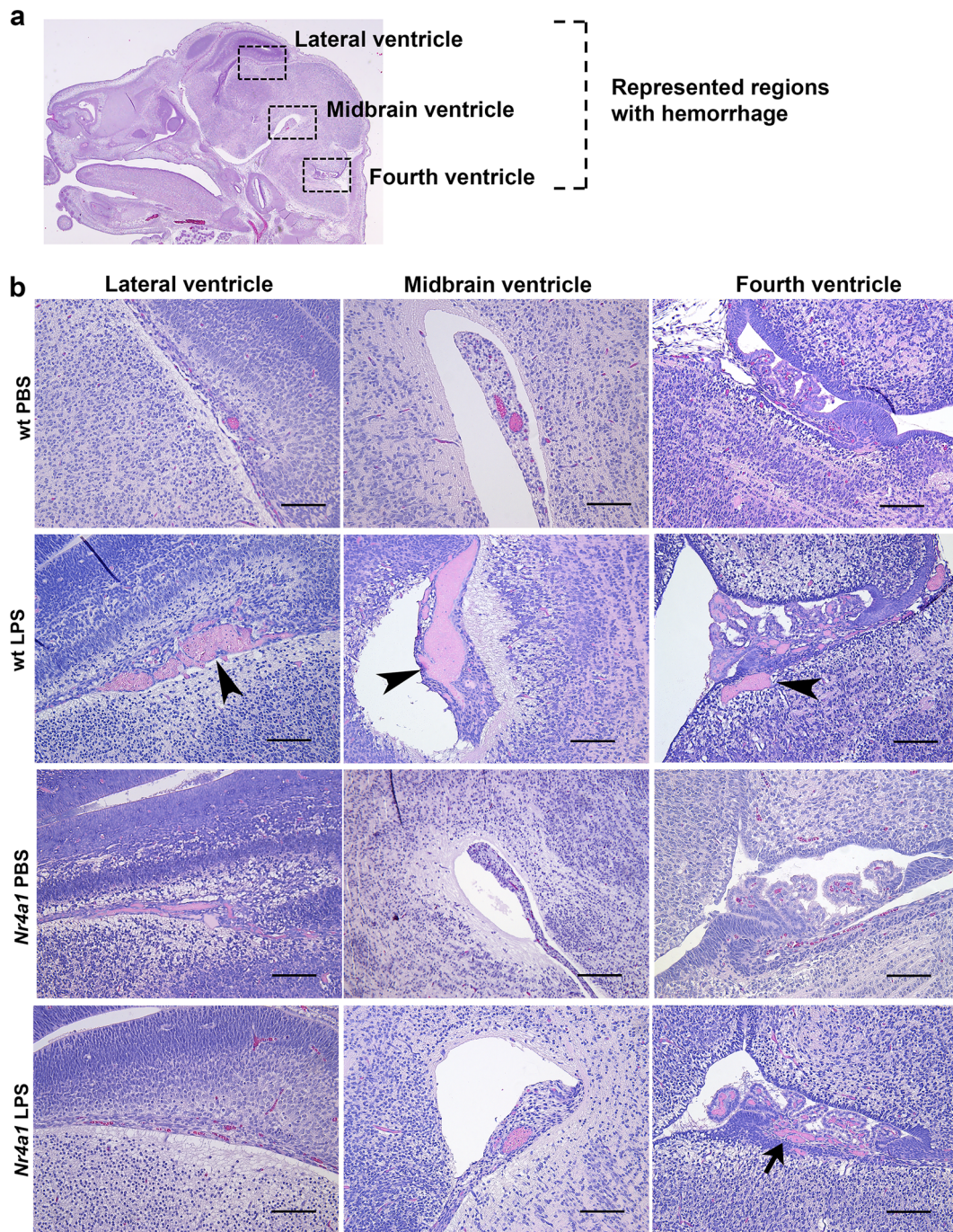
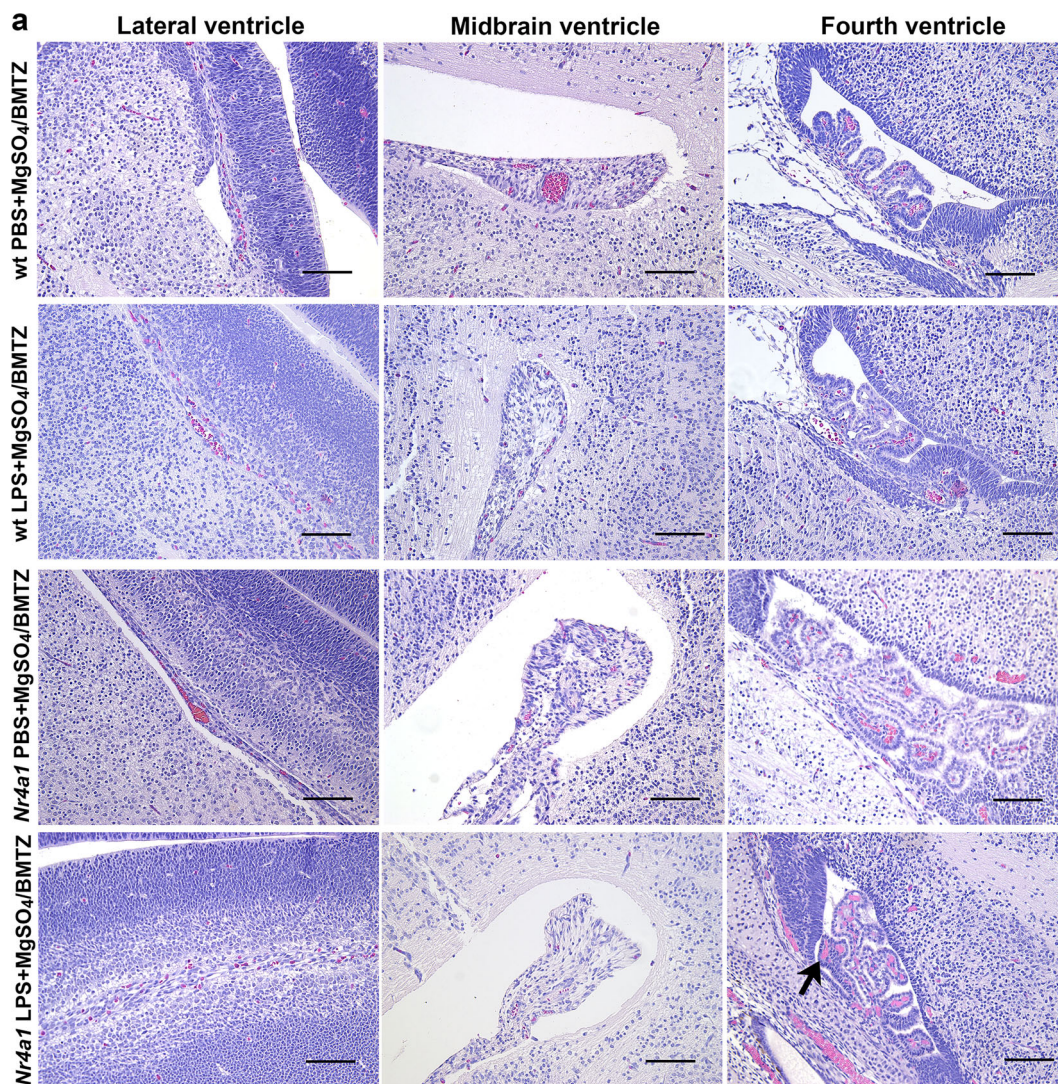


Fig. 4 Comparison of cerebral pathology observed in wt and *Nr4a1* KO embryos. **a** H&E stained cross-section of an E15.5 brain, highlighting the regions (boxed areas) where injury in the form of hemorrhage was mainly observed. **b** Representative micrographs of hemorrhage in the respective areas described in **a** for group 1 (PBS vs. LPS). Hemorrhage was predominant in wt brains exposed to LPS (arrowheads) and to a lesser extent in *Nr4a1* KO brains also exposed to LPS (arrow). Scale bars denote 100 μ m.

MgSO₄/BMTZ treatment, the number of Iba1⁺ cells in wt brains was higher but not significantly with LPS vs. PBS controls (Fig. 3b). There was also no significant difference in *Nr4a1* KO brains with MgSO₄/BMTZ treatment.

To gain more insight into the role of *Nr4a1* in perinatal brain injury, we examined the histopathology in wt versus mutant embryo brains. Most obvious was cerebral hemorrhage, occurring predominantly in the lateral ventricle, midbrain, and fourth ventricle (Fig. 4a). This



b Percentage of brains with hemorrhage

Group 1				Group 2			
	wt	<i>Nr4a1</i> KO	p-value		wt	<i>Nr4a1</i> KO	p-value
PBS	13% (1/8)	13% (1/8)	<0.0000005	PBS+MgSO ₄ /BMTZ	17% (1/6)	13% (1/8)	<0.000005
LPS	73% (8/11)	31% (4/13)		LPS+MgSO ₄ /BMTZ	17% (1/6)	33% (2/6)	

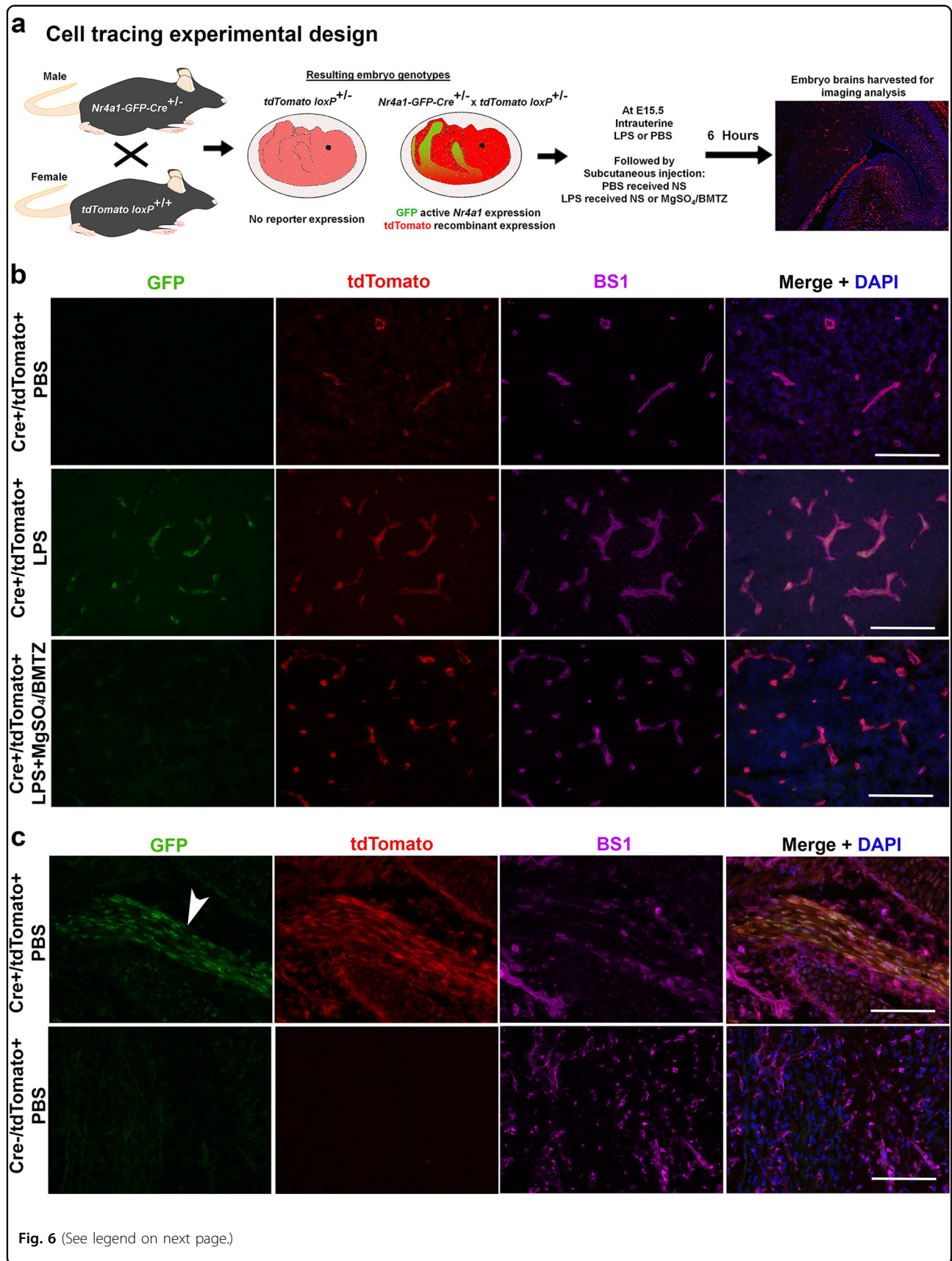
Fig. 5 Reductions of cerebral pathology in *Nr4a1* KO embryos. **a** Representative micrographs of hemorrhage (arrow), in respective areas for group 2 (PBS vs. LPS with MgSO₄/BMTZ). Scale bars denote 100 μm. **b** The frequency of cerebral hemorrhage observed per condition for groups 1 and 2. The number of brains with hemorrhage vs. total examined is indicated in the brackets to the right of the percentages. *P*-values were generated by chi-squared test using the PBS or PBS + MgSO₄/BMTZ controls as a reference.

pathology was more pronounced in wt animals exposed to LPS in comparison to PBS controls and *Nr4a1* KO brains (Fig. 4b). The frequency of hemorrhage in wt mice exposed to LPS diminished with MgSO₄/BMTZ treatment (Fig. 5a). The frequency of hemorrhage was also significantly different between wt and mutant animals in both Groups 1 and 2 (Fig. 5b). Notably, the incidence of hemorrhage in *Nr4a1* KO brains exposed to LPS and

MgSO₄/BMTZ was greater versus wt counterparts and similar to mutant mice that received only LPS.

***Nr4a1* is upregulated by cerebral endothelial cells in response to neuroinflammation**

To characterize the cellular expression of *Nr4a1*, we utilized Cre-loxP fate mapping with the *Nr4a1*-GFP-Cre model. In addition to Cre, this allele expresses GFP as an



(see figure on previous page)

Fig. 6 Fate mapping *Nr4a1* expression with perinatal neuroinflammation. **a** Experimental design for combining the *Nr4a1-GFP-Cre* and *tdTomato loxP* alleles in E15.5 embryos. Males heterozygous for *Nr4a1-GFP-Cre* were timed mated with females homozygous for *tdTomato loxP* to generate embryos that harbor both alleles at a 50% Mendelian frequency. For this comparison, *tdTomato loxP* mice were given intrauterine PBS and subcutaneous NS, LPS and NS or LPS and MgSO₄/BMTZ. Embryo brains were harvested 6 h following injections for fluorescence microscopy. **b** Representative micrographs for each genotype portraying GFP (green), indicative of real-time *Nr4a1* expression, and tdTomato (red), expressed irreversibly following Cre recombination. BS1 (magenta) was used to label the vasculature. Merged images combine all three channels with DAPI (blue). **c** Positive (skeletal muscle, arrowhead) and negative controls (Cre negative littermates) confirm the specificity of the Cre-loxP combination represented in (a). Scale bars denote 100 μm.

indicator of active *Nr4a1* expression. To compare GFP and Cre labeling, *tdTomato loxP* females were mated with *Nr4a1-GFP-Cre* males and given intrauterine PBS, LPS or LPS and MgSO₄/BMTZ at E15.5 (Fig. 6a). In brains of PBS controls, we observed tdTomato localized to the vasculature (Fig. 6b). LPS exposed animals had tdTomato and GFP, both appearing localized to the cerebral vasculature. Analogous to PBS controls, we observed only tdTomato in brains exposed to LPS and MgSO₄/BMTZ. Staining with the lectin BS1 confirmed that GFP and tdTomato reporters localized to the vasculature³¹. Both GFP and tdTomato reporters were present in the developing skeletal muscle (Fig. 6c), corresponding to the known expression of *Nr4a1* in myoblasts⁵⁴. Concurrently, fluorescence for either reporter was absent in littermates negative for the *Nr4a1-GFP-Cre* allele.

Based on the pattern of cellular expression we examined *Nr4a1* KO versus wt brains (same samples used in Fig. 2) for differences in vascular genes, *Cdhr5* and *Vegfr2*. Both genes are important for endothelial integrity and angiogenesis. Therefore a difference from PBS controls may reflect intrinsic differences in vascular development that may influence the outcomes observed in *Nr4a1* KO brains with LPS exposure^{55,56}. Secondly, we sought to gain more insight into possible declines in endothelial cell integrity or number that may also occur with LPS. Expression analysis indicates no such differences even with MgSO₄/BMTZ (Fig. 7a, b).

Discussion

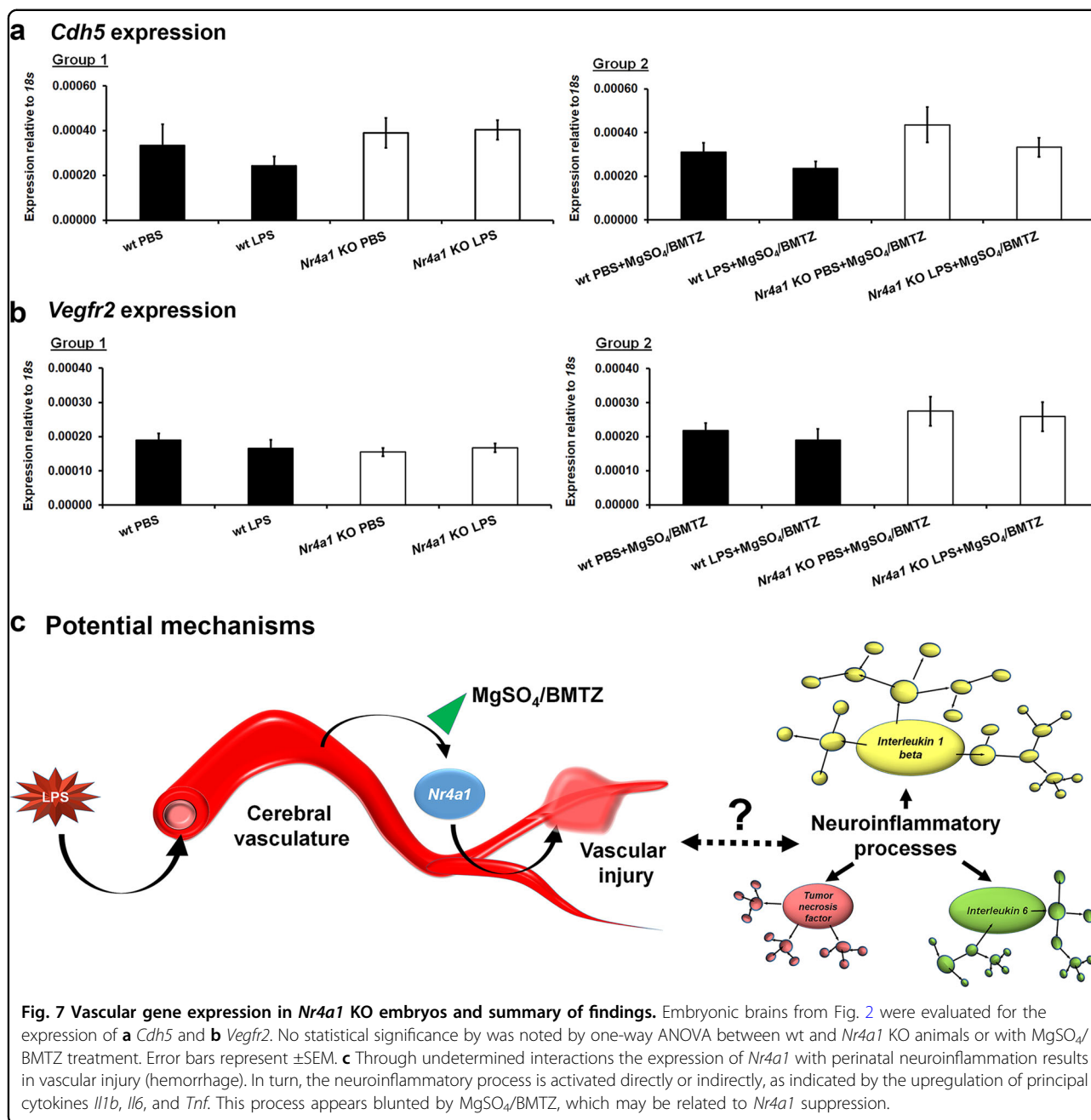
We found that *Nr4a1* is upregulated with neuroinflammation in a murine model of preterm labor. Treatments with MgSO₄/BMTZ mitigated this response in wt animals. In contrast, *Nr4a1* KO animals showed a reduction in neuroinflammation and brain injury. MgSO₄/BMTZ did not alter inflammatory responses in mutant animals. Finally, using Cre-loxP fate mapping, we were able to identify that the inflammatory upregulation of *Nr4a1* occurs in the vasculature of the fetal brain.

With normal brain development, *Nr4a1* is limited or absent according to several lines of evidence^{21,22}. In situ hybridization of fetal mouse brains show an absence of *Nr4a1* until E18.5 (© 2015 Allen Institute for Brain Science, Allen Brain Atlas API; available from:

<http://developingmouse.brain-map.org/gene/show/15145>). Within the context of preterm birth, *Nr4a1* is upregulated with lung inflammation in premature sheep⁵⁷. In addition, microarray analysis of fetal rat brains 4 h following LPS exposure reveals an increase of *Nr4a1* expression (GEO accession GDS4429)²³. This coincides with the significant increase of *Nr4a1* that we observed at 6 h following LPS. Based on this pattern of upregulation with insult, downregulation with MgSO₄/BMTZ treatments, and limited presence in brain development, we reasoned that *Nr4a1* warranted further investigation. We took a genetic approach and used an established mutant mouse model with no known developmental phenotype²². The lack of differences between PBS controls (Figs. 2–5, 7a, b) support the notion that *Nr4a1* ablation does not influence normal development. However, with the addition of an inflammatory instigator there are significant changes that may cause neurodevelopmental deficiencies noted in postnatal animals³⁶.

Our study suggest *Nr4a1* plays a prominent role in perinatal neuroinflammation and brain injury. Conversely, *Nr4a1* has been implicated in both anti- and pro-inflammatory processes. Within the adult innate immune system and with metabolic disease, *Nr4a1* plays an anti-inflammatory role^{58,59}. The mechanisms by which *Nr4a1* reduces inflammation have been noted to involve p38, NF-κB, and ISG12 depending on the context of disease, biological modeling, and analyses^{19,60,61}. In-depth molecular examination suggests p38 counters *Nr4a1* in suppressing NF-κB pro-inflammatory signaling¹⁹. Whereas comparisons of animal models reveals *Nr4a1* deficient mutants exhibit greater inflammation in response to sepsis and higher mortality versus *Isg12* deficient animals⁶¹. In the adult CNS, *Nr4a1* is broadly expressed in brain tissue and involved in regulatory functions, specifically in microglia. In contrast to our results in embryonic brains, adult *Nr4a1* KO mice show elevated autoimmune inflammatory responses by microglia and T-cells^{62–64}.

In addition to the anti-inflammatory responses, there are numerous biological processes whereby *Nr4a1* is pro-inflammatory. Nr4a receptors are expressed in several immune cells to include activated macrophages²⁰. Within the context of LPS stimulation, *Nr4a1* can also promote



macrophage NF- κ B signaling⁶⁵. Other studies have indicated that *Nr4a1* does not alter immune cell responses but instead antagonizes endothelial responses to inflammation⁶⁶. In regards to the CNS, *Nr4a1* has been implicated in adult brain injury to promote neuroinflammation and cell death^{17,18}. Although these studies did not link the cerebral vasculature to *Nr4a1* signaling, it is important to note that trauma was modeled by inducing subarachnoid hemorrhage. In regard to a role within the vasculature, various modalities have implicated *Nr4a1* in regulating endothelial cell inflammation, leakiness, permeability and

dysfunction^{40,66–68}. Such studies reinforce that *Nr4a1* is dispensable for homeostasis but is important in a pathological state. This pattern of *Nr4a1* necessity makes it an ideal target for disease, since ablation in normal processes may not result in deleterious side effects.

In this study, the absence of *Nr4a1* in KO mice resulted in a significant reduction of principal pro-inflammatory markers in the E15.5 pup brains. This evidence provides a basis for the role of *Nr4a1* in regulating bacteria initiated perinatal neuroinflammation. It is possible that *Nr4a1* promotes an increase in cytokine expression from an

inflammatory insult, as displayed by the effect of LPS in the wt mice. In comparing the LPS treatment groups of the wt and the *Nr4a1* KO, the treatment of MgSO₄/BMTZ did not appear to decrease the level of inflammatory cytokine expression. This may be explained by a potential mechanism related to *Nr4a1* signaling that is essential for the neuroprotective actions of MgSO₄/BMTZ. Alternatively, in *Nr4a1* KO animals inflammation may be reduced to a threshold whereby the treatments are no longer effective. We additionally recognize that by using MgSO₄/BMTZ in combination (a clinically relevant approach), our results cannot be attributed to one of the two medications.

The upregulation of pro-inflammatory genes with LPS exposure corresponds with a greater number of microglia in wt brains. Treatment with MgSO₄/BMTZ mitigated the increase of microglia in wt embryos that was observed with LPS alone. In mutant embryos exposed to LPS, the number of microglia did not elevate or correlate with increases in pro-inflammatory gene expression. In response to inflammatory stimuli such as LPS, microglia produce cytokines including IL-1 β ⁶⁹. It is possible that the microglial inflammatory response is restricted in mutant embryos, resulting in significantly lower levels of cytokine expression vs. wt animals. Alternatively, other cell population's upregulate cytokines independent of the mutant status but to a limited degree as compared to microglia.

To further characterize the role of *Nr4a1* in perinatal brain injury, we examined the histopathology of the embryo brains. Cerebral hemorrhage was notable in wt versus *Nr4a1* KO brains with LPS. MgSO₄/BMTZ mitigated the frequency of hemorrhage in wt brains but had no effect in KO animals. These results correspond with the pathological findings in humans, whereby the incidence of intraventricular hemorrhage is greater with prematurity and reduced by corticosteroids^{70–72}. The mechanisms of perinatal hemorrhage within the context of preterm labor are not clear. Our examination of key vascular genes suggests that cerebral hemorrhage is not a result of endothelial cell decline (Fig. 7a, b). Both MgSO₄ and corticosteroids are known to relax the vasculature^{73,74}. However, it is unclear whether vasodilation or other responses invoked by MgSO₄ and/or BMTZ confer neuroprotection. Our results suggest a possible role of *Nr4a1* with regard to MgSO₄/BMTZ and the cerebral vasculature. This is supported by the upregulation of *Nr4a1* in vessels observed with Cre-loxP fate mapping.

Whether *Nr4a1* signaling directly or indirectly influences the perinatal inflammatory response remains a question. Given that *Nr4a1* is expressed in the vasculature, we suspect that it is mediating inflammation as summarized in Fig. 7c. One of the principal inflammatory markers, *Il1b*, was intimately affected by the knockout status and the treatment group. This suggests that *Il1b*

expression is modulated by *Nr4a1*. However, it is unclear whether the upregulation of inflammatory cytokines by *Nr4a1* is direct or indirect. Vascular cells are known to express interleukin receptors and respond to inflammatory cytokines⁷⁵. Therefore, it is likely that perinatal vascular cells interact with immune cells, but are not the main source of inflammatory cytokines.

Our study's strengths include the use of multiple murine models including outbred CD1, inbred C57BL/6 and *Nr4a1* KO mice, to support our findings. Furthermore, several assays and validation experiments were conducted including the use of Cre-loxP mutants that not only substantiated the upregulation of *Nr4a1* with neuroinflammation but also implicated the vasculature. Finally, the comparison of MgSO₄/BMTZ provides additional insight into the mechanisms of neuroprotection and the role of *Nr4a1*.

The primary limitation of our study is the reliance on a mouse model of preterm labor. The mechanisms of preterm labor in humans are complex and difficult to translate. Therefore, we used an inflammation-based model which has been well described in the literature. Although other exposure modalities using live bacteria exist, we used the *in utero* LPS approach to examine specific inflammatory components of brain injury to evaluate potential mechanisms of MgSO₄/BMTZ neuroprotection^{2,51,76}.

A second limitation is the use of the microarray only for screening genes but not for functional analysis. This is due to the low number of genes that were validated; only four of our top ten were significant by qRT-PCR (Fig. 1c). Based on the high level of false positives, we deemed the microarray unsuitable for making interpretations regarding the status of the transcriptome.

A third limitation is that we could not establish a clear link between *Nr4a1* and its mechanism of action. We suspect that the mechanisms of *Nr4a1* are directly related to the vasculature and the pathology of hemorrhage. However, we could not pinpoint the role of *Nr4a1* to specific pathways within the neuroinflammatory milieu. We observed that *Nr4a1* is re-expressed in the context of neuroinflammation but the exact timing and reason for expression earlier in development also remain unclear. Finally, the etiology of preterm labor in humans is multifactorial and our observations may represent only one of many pathways that govern neuroinflammation and/or MgSO₄/BMTZ neuroprotection⁷⁷.

In closing, we have identified *Nr4a1* as a potent mediator of perinatal neuroinflammation and direct or indirect target of MgSO₄/BMTZ treatments. *Nr4a1* expression was upregulated in the fetal brain vasculature and linked to cerebral hemorrhage. The lack of *Nr4a1* in normal brains presents an opportunity to target neuroinflammation, potentially with few developmental side effects.

Based on these findings, additional studies are warranted to better understand the role of the vasculature and *Nr4a1* signaling within the context of preterm labor.

Acknowledgements

Funding for this research was provided by the U.S. Air Force SG5 award program and by Madigan Army Medical Center. We are also grateful for the support from the Madigan Laboratory Animal Resource Service, in particular by Joanna Dandeneau.

Author details

¹Department of Obstetrics and Gynecology, Division of Maternal Fetal Medicine, Madigan Army Medical Center, Tacoma, WA, USA. ²Department of Clinical Investigation, Madigan Army Medical Center, Tacoma, WA, USA. ³PharmaWrite Medical Communications LLC, Princeton, NJ, USA. ⁴Integrated Research Center for Fetal Medicine, Johns Hopkins University School of Medicine, Baltimore, MD, USA. ⁵Department of Obstetrics and Gynecology, University of Washington Medical Center, Seattle, WA, USA

Competing interests

Authors S.M.E., A.S.T., P.G.N., and N.I. have filed a provisional patent related to the targeting of *Nr4a1* for reducing neuroinflammation with preterm labor. The authors have not received any monetary benefits for this filing or have any conflicts of interest regarding this research study to declare. Funding agencies had no influence on the bearing of this study.

Disclaimer

Some authors are federal employees or members of the armed forces. The views expressed are those of the authors and do not reflect the official policy or position of the U.S. Army Medical Department, Department of the Army, Department of Defense or the U.S. Government. Animals involved in this study were maintained in accordance with the 'Guide for the Care and Use of Laboratory Animals' published by the National Research Council/Institute of Laboratory Animal Research (ILAR).

Publisher's note

Springer Nature remains neutral with regard to jurisdictional claims in published maps and institutional affiliations.

Supplementary Information accompanies this paper at (<https://doi.org/10.1038/s41419-019-2196-7>).

Received: 13 September 2019 Revised: 6 December 2019 Accepted: 9 December 2019

Published online: 06 January 2020

References

- Martin, J. A. & Osterman, M. J. K. Describing the Increase in Preterm Births in the United States, 2014–2016. *NCHS Data Brief*, 1–8 (2018).
- Burd, I., Balakrishnan, B. & Kannan, S. Models of fetal brain injury, intrauterine inflammation, and preterm birth. *Am. J. Reprod. Immunol.* **67**, 287–294 (2012).
- Yoon, B. H. et al. Fetal exposure to an intra-amniotic inflammation and the development of cerebral palsy at the age of three years. *Am. J. Obstet. Gynecol.* **182**, 675–681 (2000).
- Wood, N. S., Marlow, N., Costeloe, K., Gibson, A. T. & Wilkinson, A. R. Neurologic and developmental disability after extremely preterm birth. EPICure Study Group. *N. Engl. J. Med.* **343**, 378–384 (2000).
- Marlow, N., Wolke, D., Bracewell, M. A., Samara, M. & Group, E. P. S. Neurologic and developmental disability at six years of age after extremely preterm birth. *N. Engl. J. Med.* **352**, 9–19 (2005).
- Pierre, W. C. et al. Neonatal microglia: the cornerstone of brain fate. *Brain, Behav., Immun.* **59**, 333–345 (2017).
- Rouse, D. J. et al. A randomized, controlled trial of magnesium sulfate for the prevention of cerebral palsy. *N. Engl. J. Med.* **359**, 895–905 (2008).
- Rouse, D. J. & Hirtz, D. Eunice Kennedy Shriver National Institute of Child, H. & Human Development Maternal-Fetal Medicine Units, N. What we learned about the role of antenatal magnesium sulfate for the prevention of cerebral palsy. *Semin. Perinatol.* **40**, 303–306 (2016).
- Crowther, C. A., Hillier, J. E., Doyle, L. W. & Haslam, R. R. Australasian Collaborative Trial of Magnesium Sulphate Collaborative, G. Effect of magnesium sulfate given for neuroprotection before preterm birth: a randomized controlled trial. *JAMA* **290**, 2669–2676 (2003).
- Marret, S. et al. Magnesium sulphate given before very-preterm birth to protect infant brain: the randomised controlled PREMAG trial*. *BJOG* **114**, 310–318 (2007).
- Mittendorf, R. et al. Association between the use of antenatal magnesium sulfate in preterm labor and adverse health outcomes in infants. *Am. J. Obstet. Gynecol.* **186**, 1111–1118 (2002).
- Conde-Agudelo, A. & Romero, R. Antenatal magnesium sulfate for the prevention of cerebral palsy in preterm infants less than 34 weeks' gestation: a systematic review and metaanalysis. *Am. J. Obstet. Gynecol.* **200**, 595–609 (2009).
- Costantine, M. M. & Weiner, S. J. Eunice Kennedy Shriver National Institute of Child Health and Human Development Maternal-Fetal Medicine Units Network. Effects of antenatal exposure to magnesium sulfate on neuroprotection and mortality in preterm infants: a meta-analysis. *Obstet. Gynecol.* **114**, 354–364 (2009).
- Baud, O. et al. Antenatal glucocorticoid treatment and cystic periventricular leukomalacia in very premature infants. *N. Engl. J. Med.* **341**, 1190–1196 (1999).
- Crowley, P., Chalmers, I. & Keirse, M. J. The effects of corticosteroid administration before preterm delivery: an overview of the evidence from controlled trials. *Br. J. Obstet. Gynaecol.* **97**, 11–25 (1990).
- Coutinho, A. E. & Chapman, K. E. The anti-inflammatory and immunosuppressive effects of glucocorticoids, recent developments and mechanistic insights. *Mol. Cell. Endocrinol.* **335**, 2–13 (2011).
- Dai, Y. et al. Cyclosporin A ameliorates early brain injury after subarachnoid hemorrhage through inhibition of a Nur77 dependent apoptosis pathway. *Brain Res.* **1556**, 67–76 (2014).
- Dai, Y. et al. Nuclear receptor nur77 promotes cerebral cell apoptosis and induces early brain injury after experimental subarachnoid hemorrhage in rats. *J. Neurosci. Res.* **92**, 1110–1121 (2014).
- Li, L. et al. Impeding the interaction between Nur77 and p38 reduces LPS-induced inflammation. *Nat. Chem. Biol.* **11**, 339–346 (2015).
- Pei, L., Castrillo, A., Chen, M., Hoffmann, A. & Tontonoz, P. Induction of NR4A orphan nuclear receptor expression in macrophages in response to inflammatory stimuli. *J. Biol. Chem.* **280**, 29256–29262 (2005).
- Zetterstrom, R. H., Williams, R., Perlmann, T. & Olson, L. Cellular expression of the immediate early transcription factors Nurr1 and NGFI-B suggests a gene regulatory role in several brain regions including the nigrostriatal dopamine system. *Brain Res. Mol. Brain Res.* **41**, 111–120 (1996).
- Lee, S. L. et al. Unimpaired thymic and peripheral T cell death in mice lacking the nuclear receptor NGFI-B (Nur77). *Science* **269**, 532–535 (1995).
- Oskvig, D. B., Elkahoun, A. G., Johnson, K. R., Phillips, T. M. & Herkenham, M. Maternal immune activation by LPS selectively alters specific gene expression profiles of interneuron migration and oxidative stress in the fetus without triggering a fetal immune response. *Brain, Behav., Immun.* **26**, 623–634 (2012).
- Elovitz, M. A., Wang, Z., Chien, E. K., Rychlik, D. F. & Phillippe, M. A new model for inflammation-induced preterm birth: the role of platelet-activating factor and Toll-like receptor-4. *Am. J. Pathol.* **163**, 2103–2111 (2003).
- Hallak, M. Effect of parenteral magnesium sulfate administration on excitatory amino acid receptors in the rat brain. *Magnes. Res.* **11**, 117–131 (1998).
- Burd, I., Breen, K., Friedman, A., Chai, J. & Elovitz, M. A. Magnesium sulfate reduces inflammation-associated brain injury in fetal mice. *Am. J. Obstet. Gynecol.* **202**, 292 e291–299 (2010).
- Nadeau-Vallee, M. et al. Novel noncompetitive IL-1 receptor-biased ligand prevents infection- and inflammation-induced preterm birth. *J. Immunol.* **195**, 3402–3415 (2015).
- Wang, X. et al. Disruption of interleukin-18, but not interleukin-1, increases vulnerability to preterm delivery and fetal mortality after intrauterine inflammation. *Am. J. Pathol.* **169**, 967–976 (2006).
- Moran, A. E. et al. T cell receptor signal strength in Treg and iNKT cell development demonstrated by a novel fluorescent reporter mouse. *J. Exp. Med.* **208**, 1279–1289 (2011).
- Madisen, L. et al. A robust and high-throughput Cre reporting and characterization system for the whole mouse brain. *Nat. Neurosci.* **13**, 133–140 (2010).

31. Ieronimakis, N. et al. Coronary adventitial cells are linked to perivascular cardiac fibrosis via TGFbeta1 signaling in the mdx mouse model of Duchenne muscular dystrophy. *J. Mol. Cell. Cardiol.* **63**, 122–134 (2013).
32. Qu, Y., He, F. & Chen, Y. Different effects of the probe summarization algorithms PLIER and RMA on high-level analysis of Affymetrix exon arrays. *BMC Bioinforma.* **11**, 211 (2010).
33. Hochberg, Y. & Benjamini, Y. More powerful procedures for multiple significance testing. *Stat. Med.* **9**, 811–818 (1990).
34. Reiner, A., Yekutieli, D. & Benjamini, Y. Identifying differentially expressed genes using false discovery rate controlling procedures. *Bioinformatics* **19**, 368–375 (2003).
35. Au, C. G. et al. Increased connective tissue growth factor associated with cardiac fibrosis in the mdx mouse model of dystrophic cardiomyopathy. *Int. J. Exp. Pathol.* **92**, 57–65 (2011).
36. Thagard, A. S. et al. Long-term impact of intrauterine neuroinflammation and treatment with magnesium sulphate and betamethasone: Sex-specific differences in a preterm labor murine model. *Sci. Rep.* **7**, 17883 (2017).
37. Ye, J. et al. Primer-BLAST: a tool to design target-specific primers for polymerase chain reaction. *BMC Bioinforma.* **13**, 134 (2012).
38. Wang, X., Spandidos, A., Wang, H. & Seed, B. PrimerBank: a PCR primer database for quantitative gene expression analysis, 2012 update. *Nucleic Acids Res.* **40**, D1144–1149 (2012).
39. Winkler, D. T. et al. Spontaneous hemorrhagic stroke in a mouse model of cerebral amyloid angiopathy. *J. Neurosci.* **21**, 1619–1627 (2001).
40. Goddard, L. M. et al. Progesterone receptor in the vascular endothelium triggers physiological uterine permeability preimplantation. *Cell* **156**, 549–562 (2014).
41. Martinez-Gonzalez, J. & Badimon, L. The NR4A subfamily of nuclear receptors: new early genes regulated by growth factors in vascular cells. *Cardiovascular Res.* **65**, 609–618 (2005).
42. Quintero-Ronderos, P. & Laissue, P. The multisystemic functions of FOXD1 in development and disease. *J. Mol. Med.* **96**, 725–739 (2018).
43. Chen, J. et al. Diversification and molecular evolution of ATOH8, a gene encoding a bHLH transcription factor. *PLoS ONE* **6**, e23005 (2011).
44. Kageyama, R., Shimajo, H. & Ohtsuka, T. Dynamic control of neural stem cells by bHLH factors. *Neurosci. Res.* **138**, 12–18 (2019).
45. Krupnik, V. E. et al. Functional and structural diversity of the human Dickkopf gene family. *Gene* **238**, 301–313 (1999).
46. Anholt, R. R. Olfactomedin proteins: central players in development and disease. *Front. cell developmental Biol.* **2**, 6 (2014).
47. Sia, G. M., Clem, R. L. & Huganir, R. L. The human language-associated gene SRPX2 regulates synapse formation and vocalization in mice. *Science* **342**, 987–991 (2013).
48. Grunnet, M. et al. KCNE4 is an inhibitory subunit to Kv1.1 and Kv1.3 potassium channels. *Biophysical J.* **85**, 1525–1537 (2003).
49. Rui, X., Tsao, J., Scheys, J. O., Hammer, G. D. & Schimmer, B. P. Contributions of specificity protein-1 and steroidogenic factor 1 to Adcy4 expression in Y1 mouse adrenal cells. *Endocrinology* **149**, 3668–3678 (2008).
50. Blaho, V. A. & Hla, T. An update on the biology of sphingosine 1-phosphate receptors. *J. Lipid Res.* **55**, 1596–1608 (2014).
51. Burd, I. et al. Inflammation-induced preterm birth alters neuronal morphology in the mouse fetal brain. *J. Neurosci. Res.* **88**, 1872–1881 (2010).
52. Lei, J. et al. Maternal dendrimer-based therapy for inflammation-induced preterm birth and perinatal brain injury. *Sci. Rep.* **7**, 6106 (2017).
53. Eloundou, S. N. et al. Placental malperfusion in response to intrauterine inflammation and its connection to fetal sequelae. *PLoS one* **14**, e0214951 (2019).
54. Tontonoz, P. et al. The orphan nuclear receptor Nur77 is a determinant of myofiber size and muscle mass in mice. *Mol. Cell. Biol.* **35**, 1125–1138 (2015).
55. Vestweber, D. VE-cadherin: the major endothelial adhesion molecule controlling cellular junctions and blood vessel formation. *Arterioscler Thromb. Vasc. Biol.* **28**, 223–232 (2008).
56. Lafuente, J. V., Argandona, E. G. & Mitre, B. VEGFR-2 expression in brain injury: its distribution related to brain-blood barrier markers. *J. Neural Transm. (Vienna)* **113**, 487–496 (2006).
57. Hillman, N. H., Kemp, M. W., Noble, P. B., Kallapur, S. G. & Jobe, A. H. Sustained inflation at birth did not protect preterm fetal sheep from lung injury. *Am. J. Physiol. Lung Cell. Mol. Physiol.* **305**, L446–453 (2013).
58. Hanna, R. N. et al. NR4A1 (Nur77) deletion polarizes macrophages toward an inflammatory phenotype and increases atherosclerosis. *Circ. Res.* **110**, 416–427 (2012).
59. Koenig, D. S. et al. Nuclear receptor Nur77 limits the macrophage inflammatory response through transcriptional reprogramming of mitochondrial. *Metab. Cell Rep.* **24**, 2127–2140 e2127 (2018).
60. Popichak, K. A. et al. Compensatory expression of Nur77 and Nurr1 regulates NF-kappaB-dependent inflammatory signaling in astrocytes. *Mol. Pharmacol.* **94**, 1174–1186 (2018).
61. Uhrin, P., Perkmann, T., Binder, B. & Schabbauer, G. ISG12 is a critical modulator of innate immune responses in murine models of sepsis. *Immunobiology* **218**, 1207–1216 (2013).
62. Rothe, T. et al. The nuclear receptor Nr4a1 Acts as a Microglia Rheostat and Serves as a Therapeutic Target in Autoimmune-Driven Central Nervous System Inflammation. *J. Immunol.* **198**, 3878–3885 (2017).
63. Liebmann, M. et al. Nur77 serves as a molecular brake of the metabolic switch during T cell activation to restrict autoimmunity. *Proc. Natl Acad. Sci. USA* **115**, E8017–E8026 (2018).
64. Shaked, I. et al. Transcription factor Nr4a1 couples sympathetic and inflammatory cues in CNS-recruited macrophages to limit neuroinflammation. *Nat. Immunol.* **16**, 1228–1234 (2015).
65. Pei, L., Castrillo, A. & Tontonoz, P. Regulation of macrophage inflammatory gene expression by the orphan nuclear receptor Nur77. *Mol. Endocrinol.* **20**, 786–794 (2006).
66. Hamers, A. A. et al. Limited role of nuclear receptor Nur77 in Escherichia coli-induced peritonitis. *Infect. Immun.* **82**, 253–264 (2014).
67. Zhou, H. et al. NR4A1 aggravates the cardiac microvascular ischemia reperfusion injury through suppressing FUNDC1-mediated mitophagy and promoting Mif-required mitochondrial fission by CK2alpha. *Basic Res. Cardiol.* **113**, 23 (2018).
68. You, B., Jiang, Y. Y., Chen, S., Yan, G. & Sun, J. The orphan nuclear receptor Nur77 suppresses endothelial cell activation through induction of IkappaBalpha expression. *Circ. Res.* **104**, 742–749 (2009).
69. Cunningham, C. L., Martinez-Cerdeno, V. & Noctor, S. C. Microglia regulate the number of neural precursor cells in the developing cerebral cortex. *J. Neurosci.* **33**, 4216–4233 (2013).
70. Canterino, J. C. et al. Antenatal steroids and neonatal periventricular leukomalacia. *Obstet. Gynecol.* **97**, 135–139 (2001).
71. Canterino, J. C. et al. Maternal magnesium sulfate and the development of neonatal periventricular leukomalacia and intraventricular hemorrhage. *Obstet. Gynecol.* **93**, 396–402 (1999).
72. Pinto Cardoso, G. et al. Association of intraventricular hemorrhage and death with tocolytic exposure in preterm infants. *JAMA Netw. Open* **1**, e182355 (2018).
73. Tang, J. et al. Magnesium sulfate-mediated vascular relaxation and calcium channel activity in placental vessels different from nonplacental vessels. *J. Am. Heart Assoc.* **7**, <https://doi.org/10.1161/JAHA.118.009896> (2018).
74. Deruelle, P. et al. Effects of antenatal glucocorticoids on pulmonary vascular reactivity in the ovine fetus. *Am. J. Obstet. Gynecol.* **189**, 208–215 (2003).
75. Wong, M. L. et al. IL-1 beta, IL-1 receptor type I and iNOS gene expression in rat brain vasculature and perivascular areas. *Neuroreport* **7**, 2445–2448 (1996).
76. Burd, I. et al. Beyond white matter damage: fetal neuronal injury in a mouse model of preterm birth. *Am. J. Obstet. Gynecol.* **201**, 279 e271–278 (2009).
77. Goldenberg, R. L., Culhane, J. F., Iams, J. D. & Romero, R. Epidemiology and causes of preterm birth. *Lancet* **371**, 75–84 (2008).